Supplementary Material: Separable and Semiparametric Network-based Counting Processes applied to the International Combat Aircraft Trades

Cornelius Fritz*, Paul W. Thurner†, Göran Kauermann*
Department of Statistics, LMU Munich*
Geschwister Scholl Institute of Political Science, LMU Munich†

August 16, 2021

Contents

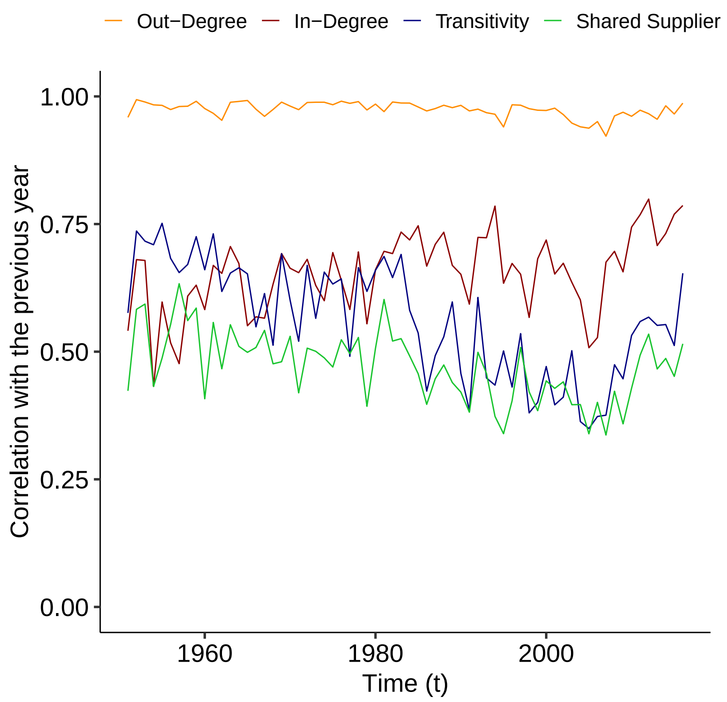

Figure 1: Yearly auto-correlations of endogenous covariates.

A Correlation of Endogenous Statistics between Subsequent Years

To further legitimize the usage of lagged endogenous covariates, we investigate the yearly auto-correlations of the corresponding statistics. Therefore, we construct time series on the monadic level for the in- and out-degrees of each country and at the dyadic level for triangular statistics, i.e., regarding a tuple of countries. In Figure 1, we then descriptively analyze the yearly correlation between all statistics, where measurements are available at both time points. The results again highlight the reliability of using the endogenous statistics of the past year as a proxy for the current year, as we observe exceptionally high correlations.

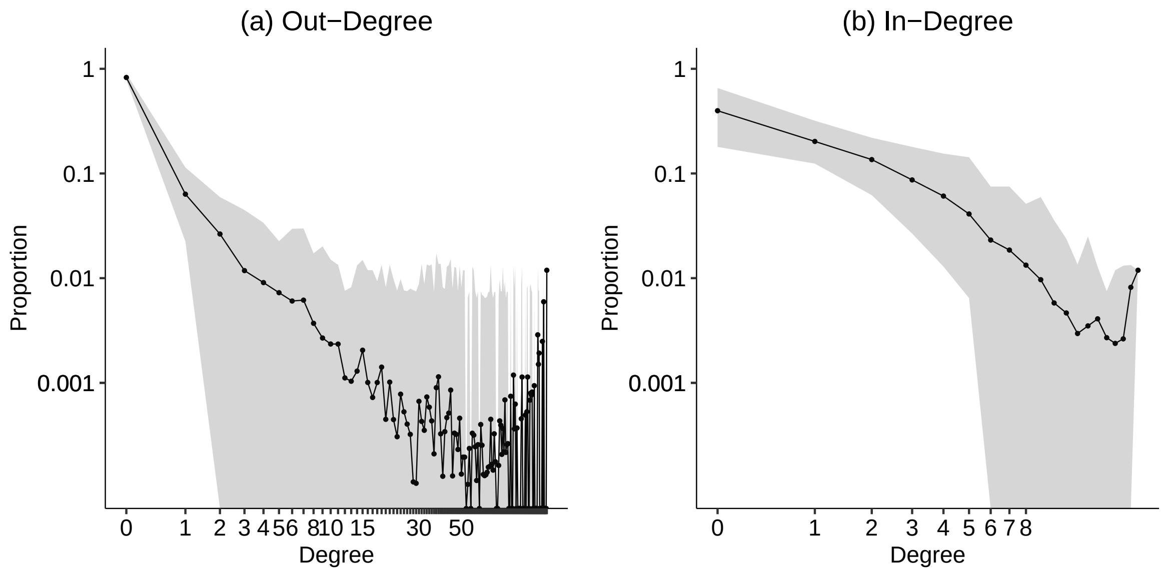

Figure 2: Average Degree Distributions of the Out- and In-Degree for all included countries. The shaded area represents the minimum and maximum observed value. All graphs are represented on a logarithmic scale.

B Data Sources

Table 1: Data sources of the exogenous covariates. Versions are indicated where available.

Covariate	From	To	Data Source
GDP, Base-Year 2005	1950	2011	Gleditsch (2002), v4.1
	2012	2017	World Bank (2017)
Military Expenditure, Base-Year 2017	1950	2000	Singer et al. (1972), v5.0
	2000	2017	SIPRI (2019)
Polity Score	1950	2017	Marshall (2017)
Alliance	1950	2017	Leeds (2019), v4.01
Distance of Capitals	1950	2017	Gleditsch (2013)

C Further Descriptive Analysis

The distribution of the in- and out-degrees can be used to analyze the topology of general networks (Barabási and Albert, 1999; Snijders, 2003; Newman et al., 2002). Similar to the findings in Figure 2 of the main article, 2 (a) underpins the strong centralization of the out-degree distribution. Again mirroring the results of the main article, the in-degree distribution is not as skewed, Figure 2 (b). There are few high degree countries, but the mode is still at zero.

Alternatively, we can focus the descriptive analysis on the top 10 sender and receiver in the network. The yearly counts of the respective countries are represented as boxplots in Figure 3 and 4. The exposed situation of USA is clearly visible, especially in Figure 3. This role was already thoroughly analyzed in Lorell (2003). India predominantly buys combat aircraft from Great Britain, which reflects the dyadic colonial history. Japan, on the other hand, obtains 95% of the delivered aircraft from USA, being the second highest receiving country.

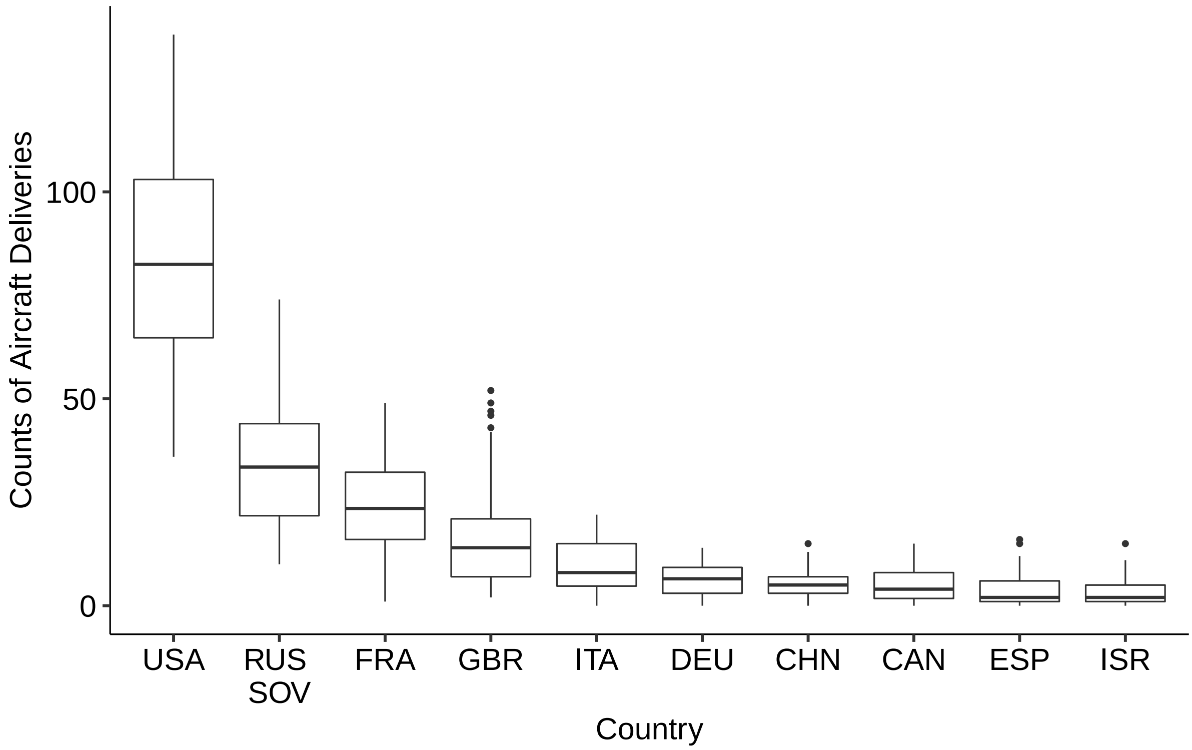

Figure 3: Boxplot of the observed counts over the years of the top 10 sender countries. The labels are the ISO3 codes of the respective countries.

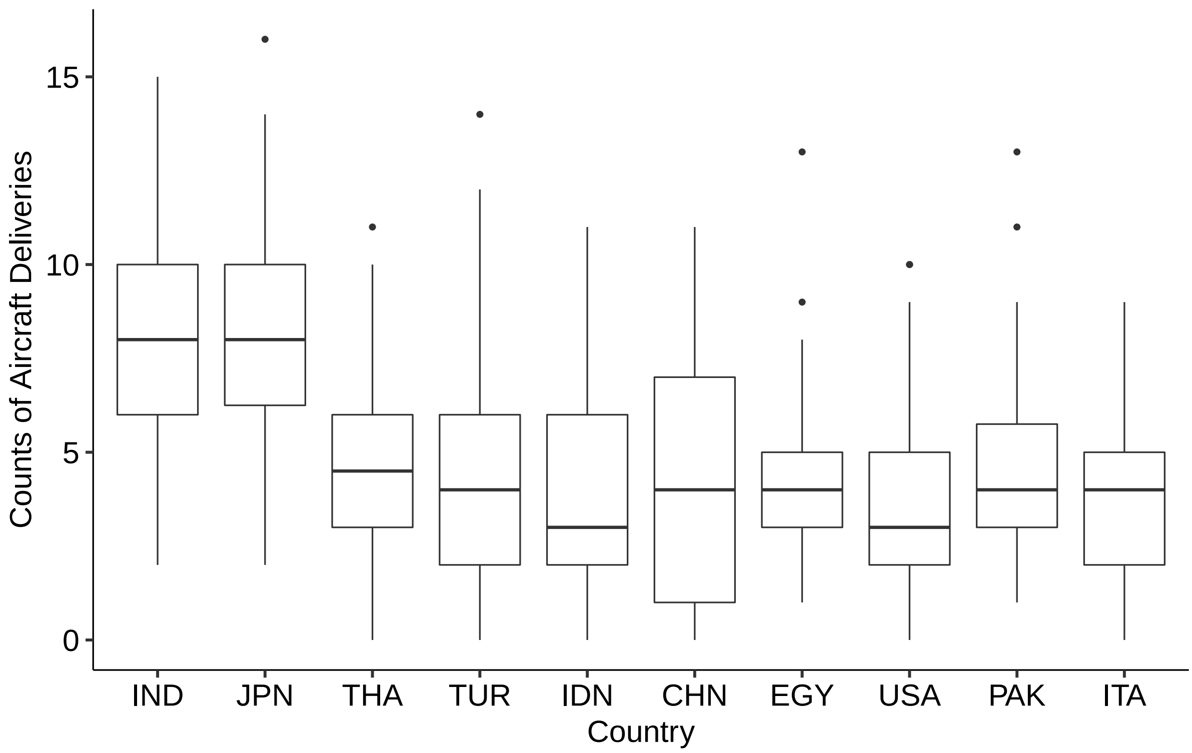

Figure 4: Boxplot of the observed counts over the years of the top 10 sender countries. The labels are the ISO3 codes of the respective countries.

D Robustness Checks

D.1 Weighted Fit

Each event can be comprehended as having a weight given by its TIV. As most possible events in out application were not realized, the respective TIVs are set to zero. Therefore, the weight of the tuple between country i and j at time point t is given by $w_{ij}(t) \propto \log\Big(\text{TIV}_{ij}(t) + 1\Big) + 1$, where $\text{TIV}_{ij}(t)$ denotes the aggregated TIVs of the same country tuple in the year t. The proportionality stems from the fact, that the weights are subsequently standardized so that their sum equals 1.

Figures 5, 6, and 7 contrast the estimates resulting from the original and weighted fit. The substantial conclusions drawn in Section 4 of the main article are paralleled by the weighted estimates.

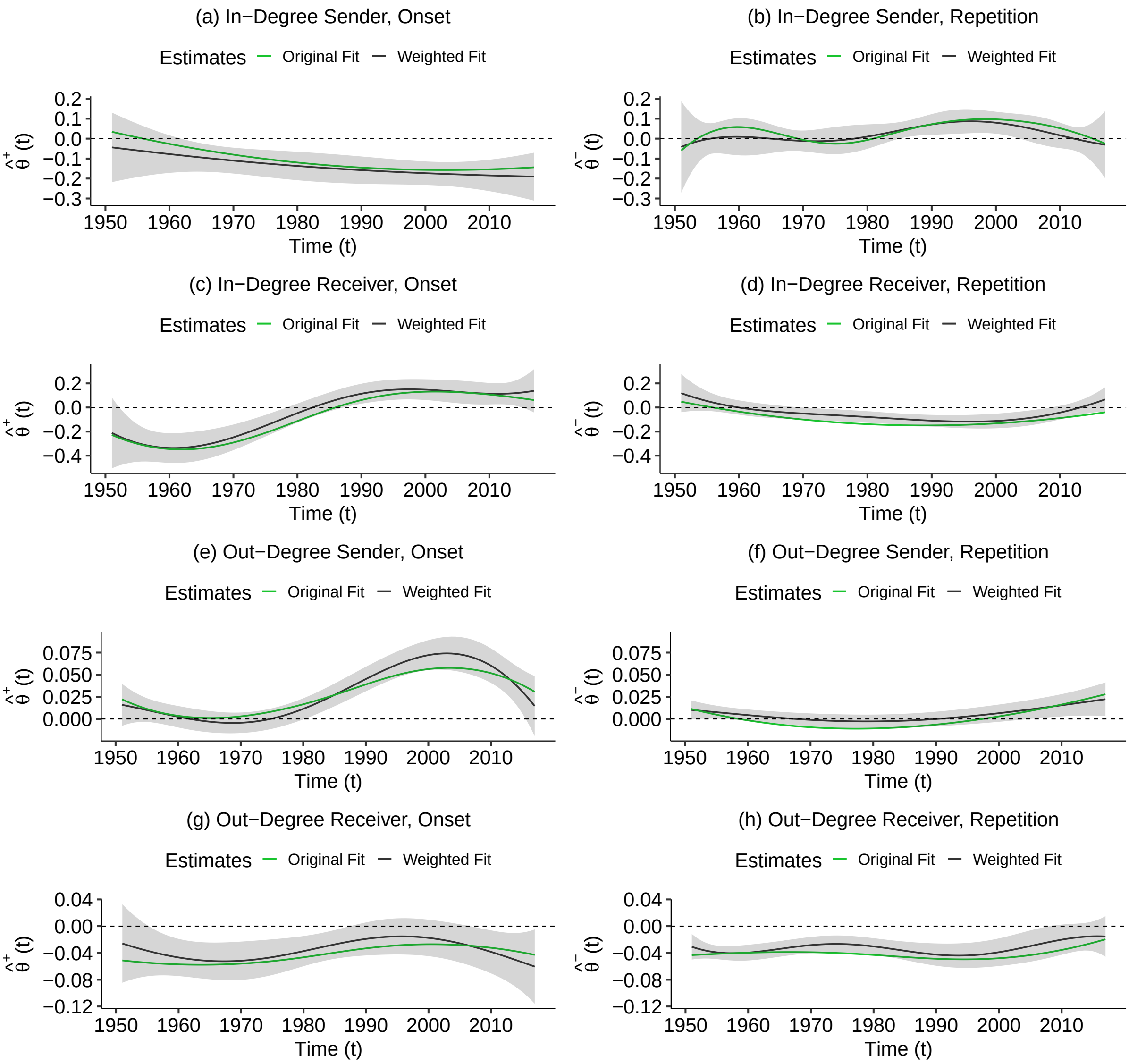

Figure 5: Robustness checks of the estimated parameters comparing the original fit to the model that weighted the observations according to the respective TIV.The green line represents the original fit, while the shaded area indicates the 95% quantile confidence bands of the weighted estimation.

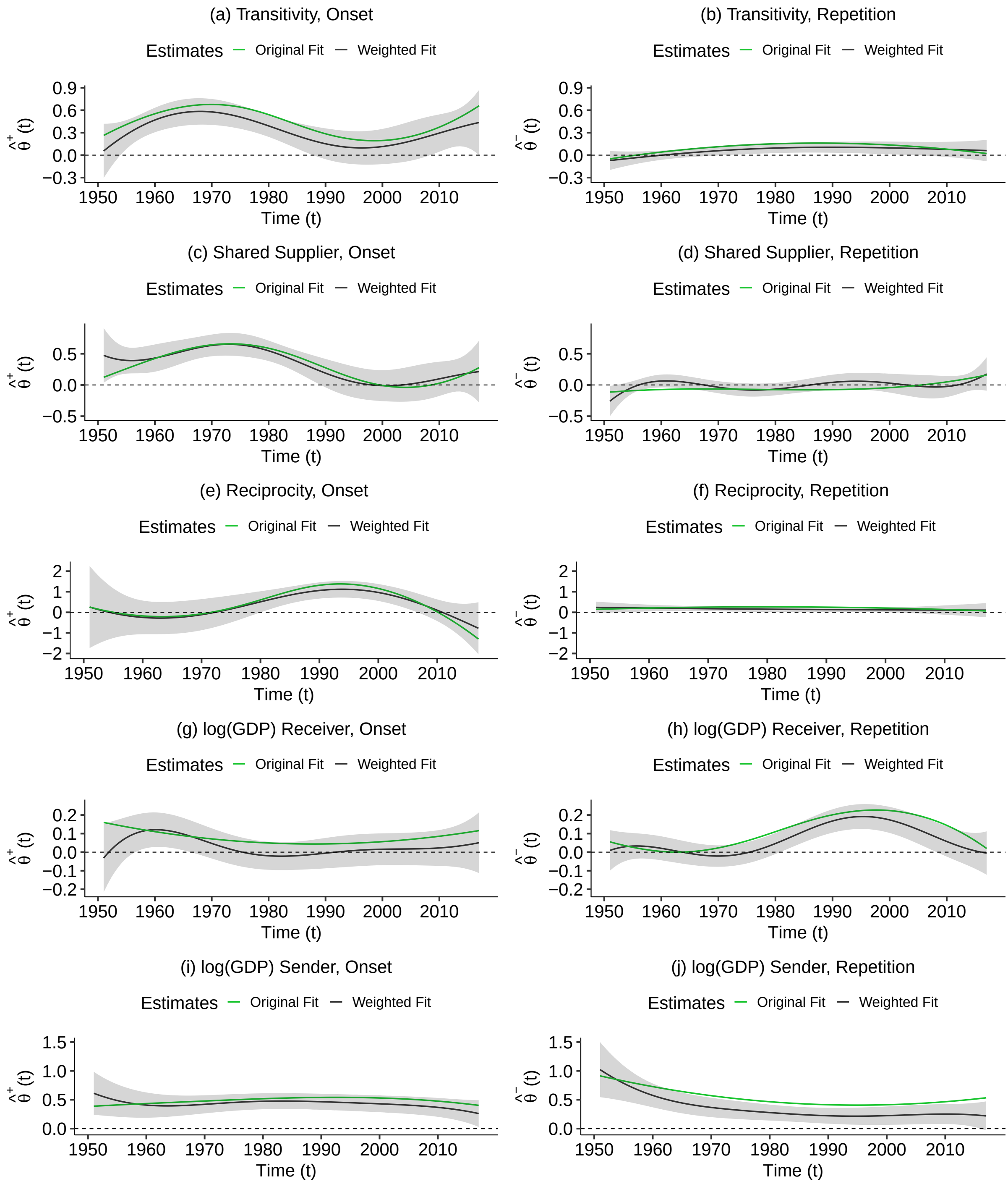

Figure 6: Robustness checks of the estimated parameters comparing the original fit to the model that weighted the observations according to the respective TIV.The green line represents the original fit, while the shaded area indicates the 95% quantile confidence bands of the weighted estimation.

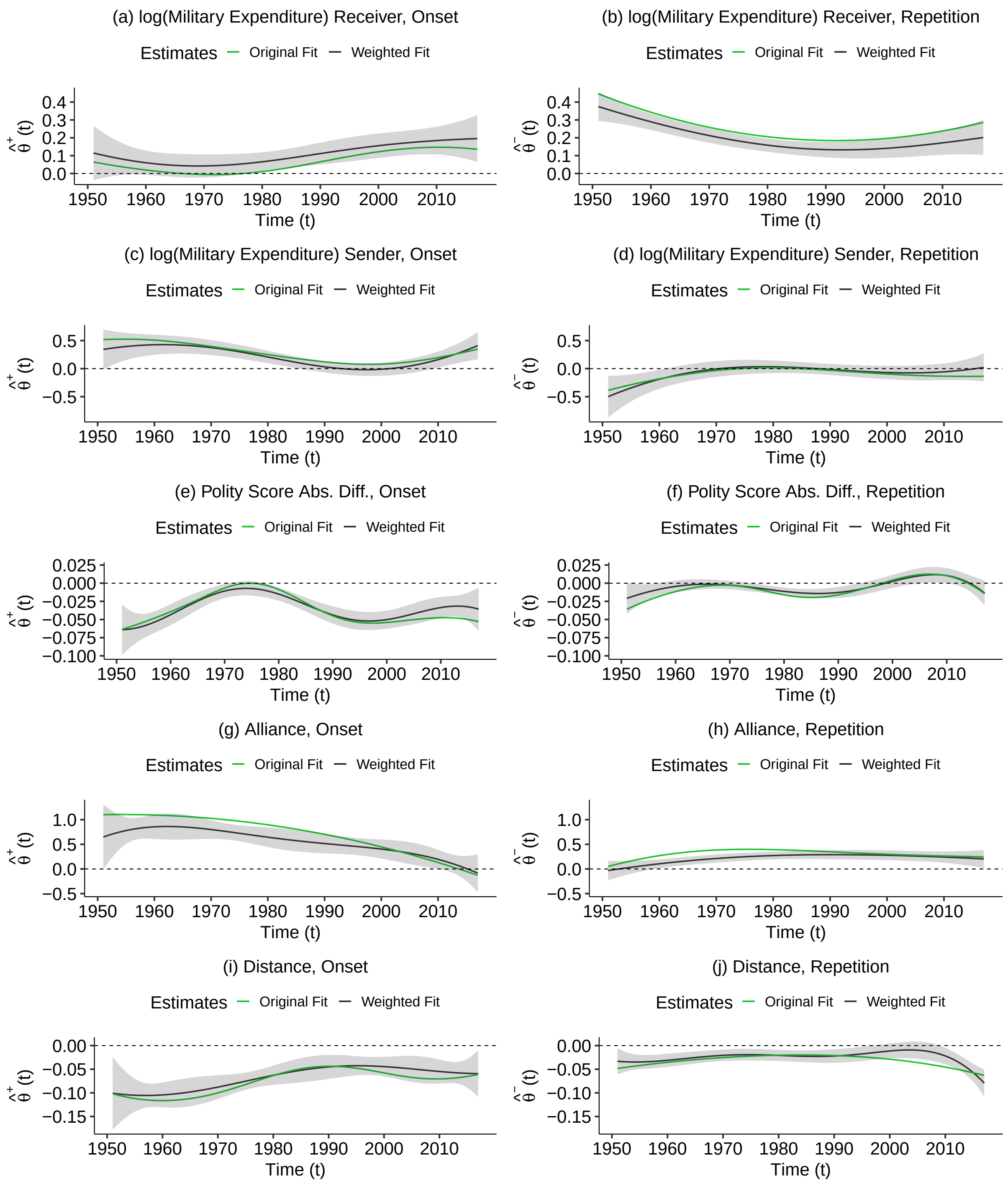

Figure 7: Robustness checks of the estimated parameters comparing the original fit to the model that weighted the observations according to the respective TIV.The green line represents the original fit, while the shaded area indicates the 95% quantile confidence bands of the weighted estimation.

D.2 Alternative Time-Spans defining Separability

The separability assumption can be adapted by changing the time frame, dictating which intensity governs which event. In the application case we fixed this interval to be one year. In order to legitimize this decision, we estimated the exact same model with a varying interval length defining from when an event tuple is, e.g., driven by the *onset* intensity.

For instance, a lag of 10 years would translate to being driving by the *onset* intensity if two countries did not trade with each other in the last 10 years. Figure 8 plots the AIC scores and values of the log likelihood evaluated at the final estimates of the respective models over the lag. Apparently, there are only slight differences between using a log of one or two years, yet longer lags lead to a steadily deteriorating performance of the model.

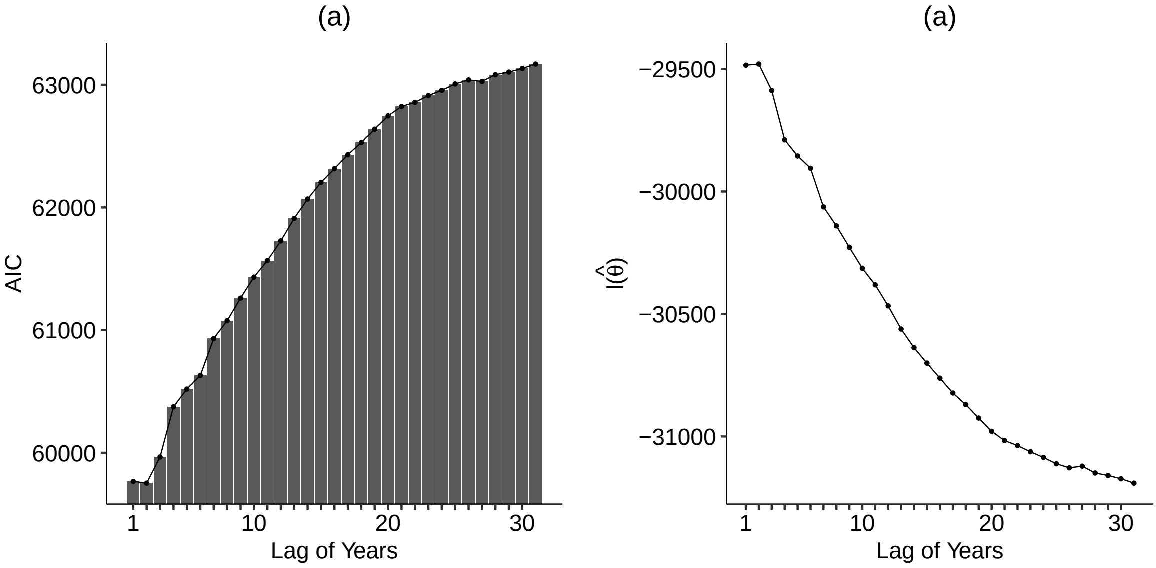

Figure 8: (a): Resulting AIC value by varying the length of the interval defining the separability. (b): The value of the log likelihood evaluated at the final estimates of the respective models.

D.3 Thresholds for TIV of Events

In the application of Section 3 all events were regarded unconditional of their extent. Alternatively, one may only include events above a certain threshold in terms of TIVs of the events. As a robustness check of the findings in the article, we, therefore, repeat the parameter estimation in three different scenarios, which are defined as follows:

1. Include events, if their TIV is above the 0.05 quantile of all TIVs ($> z_{0.05}$)
2. Include events, if their TIV is above the 0.1 quantile of all TIVs ($> z_{0.1}$)
3. Include events, if their TIV is above the 0.15 quantile of all TIVs ($> z_{0.15}$)
4. Include all events (Full Data)

The resulting estimates are shown in Figures 9 to 11 and proof the robustness of Figures 4 to 7. More specifically, equal interpretations and conclusions stated in Section 3.3.1 still hold. Only slight variations are visible in Figure 9 (g) concerning the out-degree of the receiver. Comparing the confidence bands of the original model with the estimates of the conditional models, we observe full coverage in most cases.

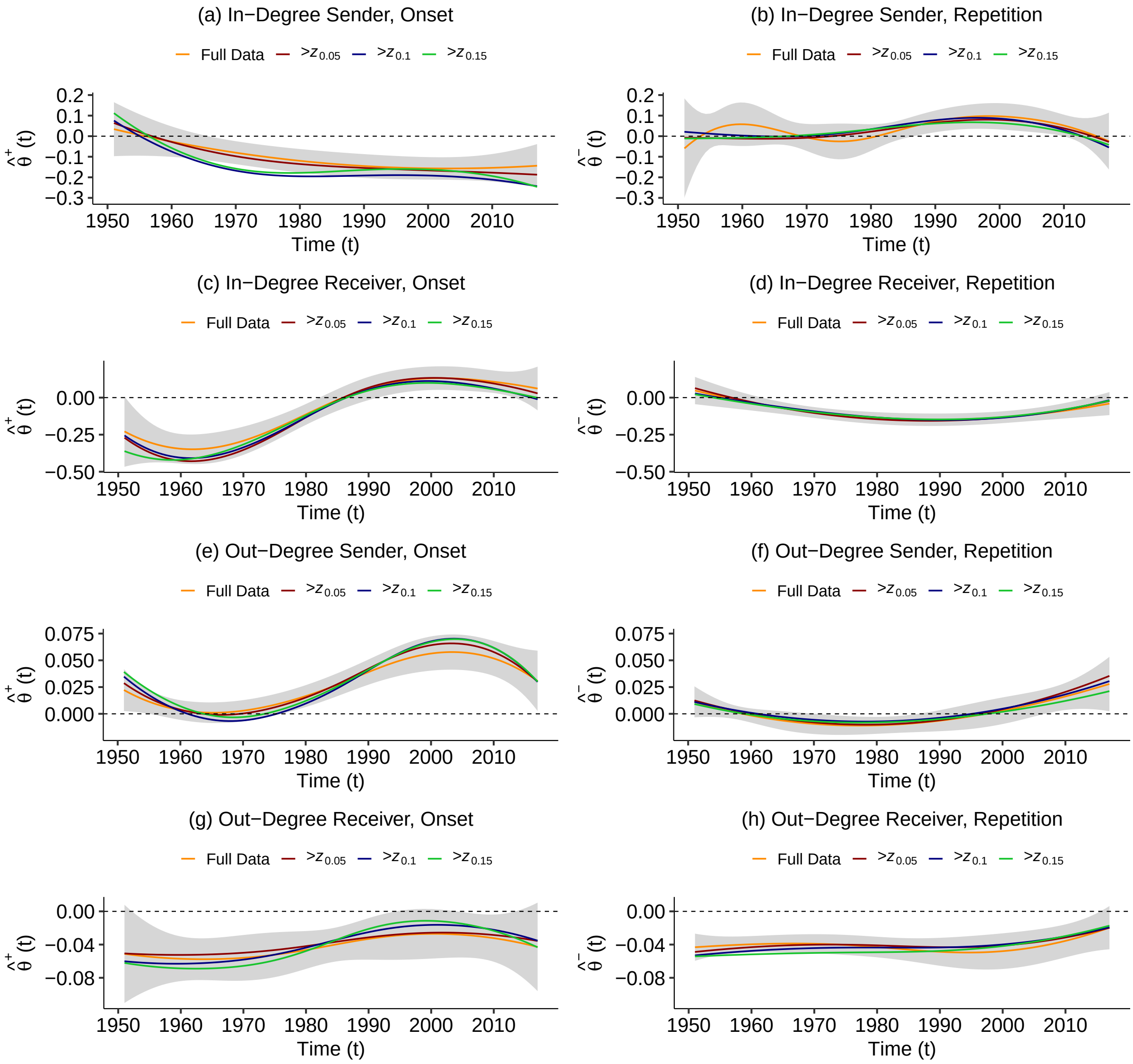

Figure 9: Robustness checks of the estimated parameters when only events with a specific TIV are regarded.The shaded area indicates the 95% confidence bands of the estimates from the unconditional model including all events.

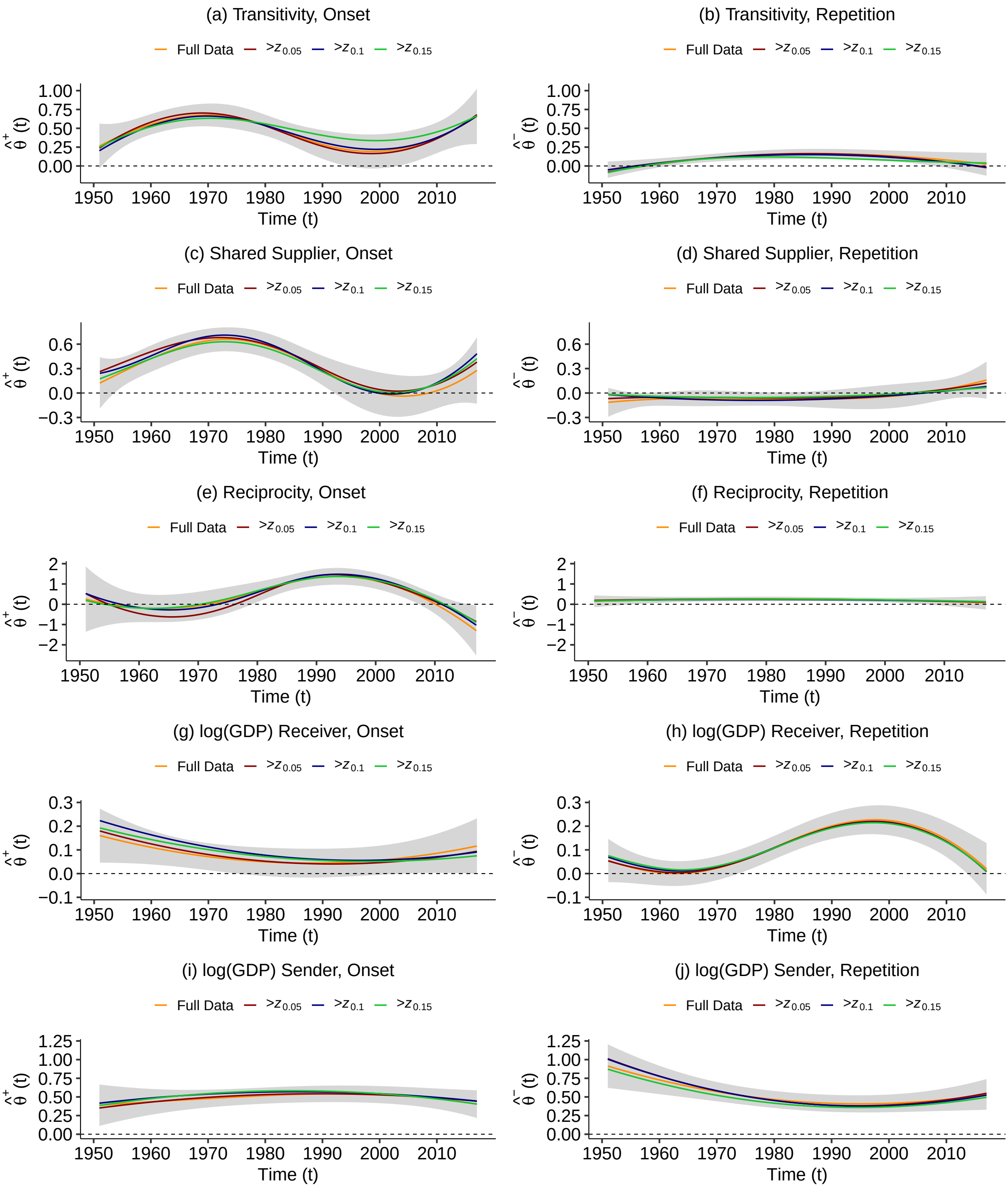

Figure 10: Robustness checks of the estimated parameters when only events with a specific TIV are regarded.The shaded area indicates the 95% confidence bands of the estimates from the unconditional model including all events.

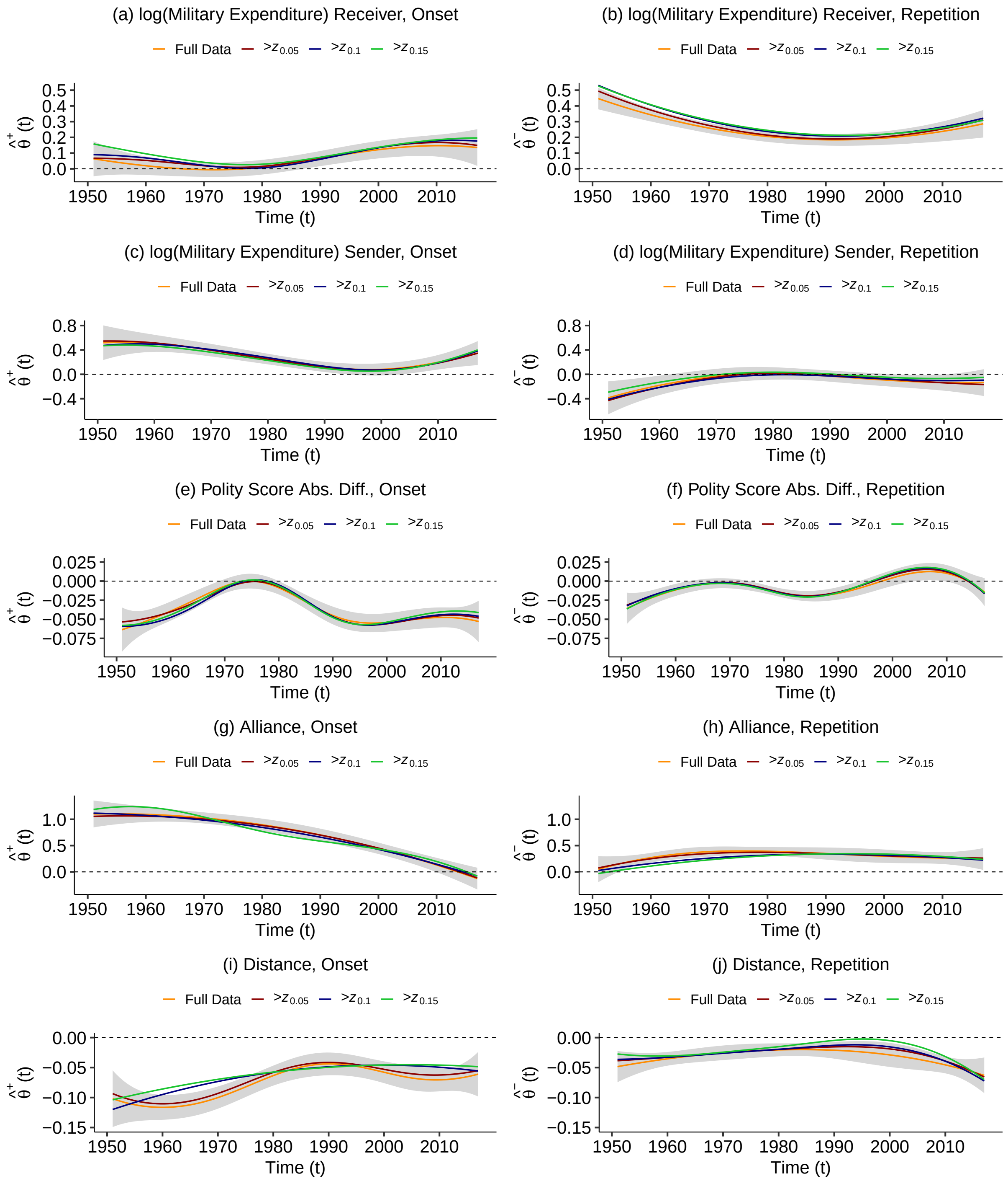

Figure 11: Robustness checks of the estimated parameters when only events with a specific TIV are regarded.The shaded area indicates the 95% confidence bands of the estimates from the unconditional model including all events.

Table 2: Specifications of the compared models and resulting corrected AIC$_c$ value.

	Separability	Time-Varying Effects	Random Effects	AIC$_c$
Model 1	✗	✗	✗	84622.47
Model 2	✓	✗	✗	65614.86
Model 3	✓	✓	✗	63174.54
Model 4	✓	✓	✓	59718.04

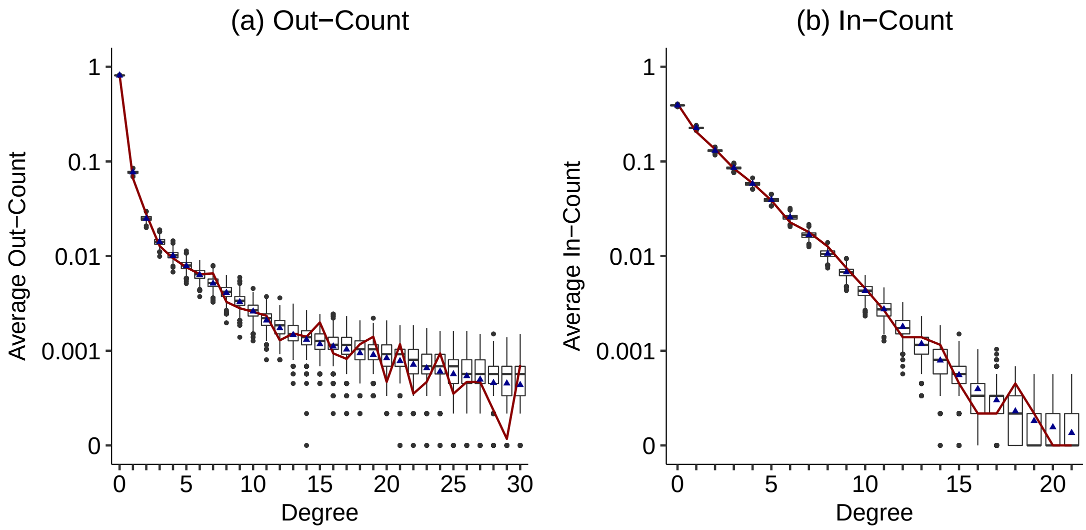

Figure 12: Comparison of the observed and simulated count distributions of the Out- (a) and In-Counts (b) for all included countries summed up over all years. The red lines indicate the observed values of each respective case, whereas the boxplots are the result of drawing 1000 networks and the blue triangles the average values.

D.4 Corrected AIC for Finite Sample Size

Besides correcting for the uncertainty resulting from estimating the variance and tuning parameters of the random and smooth components, we can define a version of the same AIC value that corrects for finite sample sizes as proposed by Hurvich and Tsai (1989). Table 2 reports this type of AIC value, although the results do not change compared to the values reported in the main article.

E Further Results of the Model Assessment

We begin by giving the mathematical formulations of the three network statistics for weighted networks analyzed in Section 3.4 of the main article. For the rootogram, we compute the frequencies h_k of combat aircraft deliveries $k \in \{1, \dots\}$ over all year. We calculated the weighted clustering coefficient proposed by Opsahl and Panzarasa (2009) for the increments of our network counting process in each year. For the increments $\boldsymbol{y}_t$ in year t, we hence count the total value of the closed triplets and all triplets and define the generalized clustering coefficient by their ratio. We specify a triplet's value as the arithmetic mean of all observed weights, i.e., the number of yearly deliveries in our application case. The in-count of all countries in year t determines the yearly average in-count. For country i the in-count in year t is defined by in-count$(i,t) = \sum_{j=1}^{n} y_{ji,t}$. Taking the arithmetic mean over all in-count(i,t) $\forall$ $i \in \mathcal{A}_t$, where the set $\mathcal{A}_t$ includes all countries present in the trade network in year t, gives the average in-count per year. The resultant statistic is proportional to the average events per year. We define the out-count in the same line. If we then concatenate all in- or out-counts over all years, the resulting empirical distribution represents the in- or out-counts irrespective of time. Figure 12 gives visual proof that our model can conserve both the in- and out-count distributions.

References

Barabási, A.-L. and Albert, R. (1999). Emergence of scaling in random networks. *Science*, 286(5439):509–512.

Gleditsch, K. S. (2002). Expanded trade and GDP data. *Journal of Conflict Resolution*, 46(5):712–724.

Gleditsch, K. S. (2013). Distance between capital cities.

Hurvich, C. M. and Tsai, C. L. (1989). Regression and time series model selection in small samples. *Biometrika*, 76(2):297–307.

Leeds, B. A. (2019). Alliance areaty obligations and provisions (ATOP 4.01). http://www.atopdata.org/ (visited 2019-09-30.

Lorell, M. A. (2003). *The U.S. combat aircraft industry, 1909-2000 : structure, competition, innovation.* RAND Corporation, Santa Monica, CA; Arlington, VA; Pittsburgh, PA.

Marshall, M. G. (2017). Polity IV project: Political regime characteristics and transitions, 1800-2016. http://www.systemicpeace.org/inscrdata.html (visited 2019-09-16).

Newman, M. E. J., Watts, D. J., and Strogatz, S. H. (2002). Random graph models of social networks. *Proceedings of the National Academy of Sciences*, 99(S 1):2566–2572.

Opsahl, T. and Panzarasa, P. (2009). Clustering in weighted networks. *Social Networks*, 31(2):155–163.

Singer, J. D., Bremer, S., and Stuckey, J. (1972). Capability distribution, uncertainty, and major power war, 1820-1965. In Russett, B., editor, *Peace, War, and Numbers*, volume 19, pages 19–48. Sage.

SIPRI (2019). Military expenditure database. https://www.sipri.org/databases/milex (visited 2020-09-03).

Snijders, T. A. B. (2003). Accounting for degree distribution in empirical analysis of network dynamics. In *Dynamic Social Network Modeling and Analysis: Workshop Summary and Papers*, pages 146–161. The National Academies Press.

World Bank (2017). World Bank Open Data.